Nucl Med Mol Imaging (2015) 49:182–190
DOI 10.1007/s13139-015-0338-0

ORIGINAL ARTICLE

ISSN (print) 1869-3474
ISSN (online) 1869-3482

Imaging Findings and Literature Review of ^{18}F-FDG PET/CT in Primary Systemic AL Amyloidosis

Joo Hee Lee[1] · Ga Yeon Lee[2] · Seok Jin Kim[2] · Ki Hyun Kim[2] · Eun-Seok Jeon[2] · Kyung-Han Lee[1] · Byung-Tae Kim[1] · Joon Young Choi[1]

Received: 18 November 2014 / Revised: 9 April 2015 / Accepted: 12 April 2015 / Published online: 13 May 2015

Abstract
Purpose Although several case reports and case series have described ^{18}F-FDG PET/CT in amyloidosis, the value of ^{18}F-FDG PET/CT for diagnosing amyloidosis has not been clarified. We investigated the imaging findings of ^{18}F-FDG PET/CT in patients with primary systemic AL amyloidosis.
Methods Subjects were 15 patients (M:F=12:3; age, 61.5± 7.4 years) with histologically confirmed primary systemic AL amyloidosis who underwent pretreatment ^{18}F-FDG PET/CT to rule out the possibility of malignancy or for initial workup of alleged cancer. For involved organs, visual and semiquantitative analyses were performed on ^{18}F-FDG PET/CT images. In total, 22 organs (10 hearts, 5 kidneys, 2 stomachs, 2 colons, 1 ileum, 1 pancreas, and 1 liver) were histologically confirmed to have primary systemic AL amyloidosis.
Results F-FDG uptake was significantly increased in 15 of the 22 organs (68.2 %; 10 hearts, 2 kidneys, 1 colon, 1 ileum, and 1 liver; SUVmax=7.0±3.2, range 2.1–14.1). However, in 11 of 15 PET-positive organs (78.6 %; 10 hearts and the ileum), it was difficult to differentiate pathological uptake from physiological uptake. Definitely abnormal ^{18}F-FDG uptake was found in only 4 of the 22 organs (18.2 %; 2 kidneys, 1 colon, and the liver). ^{18}F-FDG uptake was negative for pancreas and gastric lesions.
Conclusions Although ^{18}F-FDG PET/CT showed high uptake in two-thirds of the organs involving primary systemic AL amyloidosis, its sensitivity appeared to be low to make differentiation of pathological uptake from physiological uptake. However, due to the small number of cases, further study for the role of ^{18}F-FDG PET/CT in amyloidosis will be warranted.

Keywords ^{18}F-FDG · PET/CT · Amyloidosis · Immunoglobulin light chain amyloidosis

Introduction

Amyloidosis refers to extracellular deposition of insoluble polymeric protein fibrils in tissue and organs, resulting in damage [1]. Deposition of amyloid can be localized or systemic [2]. The most common forms of systemic amyloidosis are associated with plasma cell dyscrasias (AL and AH amyloidosis), chronic inflammation (AA amyloidosis), age (senile amyloidosis), and heredity (ATTR amyloidosis) [3]. Because clinical manifestations, treatment options and prognosis vary by subtype, the precursor protein is used to sort amyloids into the current classification of amyloidosis [4, 5]. Therefore, tissue confirmation is regarded as the "gold standard" for diagnosis [1, 4, 6]. Systemic amyloidosis is usually fatal and asymptomatic [1, 7]. Prognosis has been improved by specific treatments such as timely hemodialysis or transplantation [1]. Therefore, precise early diagnosis, exact determination of the subtype, and confirmation of the involved organs are essential for guiding patient care [5].

Because amyloid deposits are usually widespread in primary systemic AL amyloidosis, biopsy for all involved organs is an indispensable component of diagnosis. However, because of the variable and nonspecific symptoms, it is difficult to

✉ Joon Young Choi
jynm.choi@samsung.com

[1] Department of Nuclear Medicine, Samsung Medical Center, Sungkyunkwan University School of Medicine, 81 Irwon-ro, Gangnam-gu 135-710, Seoul, Republic of Korea

[2] Department of Medicine, Samsung Medical Center, Sungkyunkwan University School of Medicine, Seoul, Republic of Korea

determine how many organs are involved in individual amyloidosis cases. Moreover, even when the involved organs are known, biopsy of each could be dangerous for patients in poor general condition or when the involved organs are critical to life, such as the heart, kidneys, and lungs. Also, histology cannot provide information about the overall whole-body load, nor can it monitor the natural course of amyloidosis or the response of treatment [1].

Several non-invasive imaging modalities have been used to evaluate amyloidosis [5]. In cardiac amyloidosis, the most widely studied type, echocardiography, electrocardiograms, and magnetic resonance imaging (MRI) are all non-invasive diagnostic tools [6, 8, 9]. Chest CT is used to evaluate the characteristics of pulmonary lesions [10]. However, those imaging methods remain problematic because of nonspecific and diverse findings with various levels of diagnostic accuracy [10]. In addition, those are a regional imaging modality, not whole-body imaging.

In this respect, a whole-body functional imaging tool is warranted to represent amyloid deposition, distribution, and metabolic activity. Previous reports have identified radiotracers useful for evaluating amyloidosis such as ^{123}I-labeled serum-amyloid-P component (SAP) scintigraphy, technetium-3,3-diphosphono-1,2-pyrophosphate (^{99m}Tc-DPD) scan and *N*-[methyl-^{11}C]2-(4′-methylamino-phenyl)-6-hydroxybenzothiazole (^{11}C-PIB) PET. ^{123}I-Labeled serum-amyloid-P component (SAP) scintigraphy is a reliable tool for amyloidosis diagnosis, extension, and response evaluation, but low-quality heart visualization, high costs, and the limited availability of purified SAP and ^{123}I are major disadvantages to its use [8, 11–14]. Moreover, this method cannot apply to cardiac amyloidosis [15]. Technetium-3,3-diphosphono-1,2-pyrophosphate (^{99m}Tc-DPD) also accumulates in the myocardium in cardiac amyloidosis [5, 8]. ^{99m}Tc-DPD was particularly noted because it can distinguish between the ATTR and AL subtypes in cardiac amyloidosis [5, 8, 9]. However, a relatively small number of cases have been reported, further study will be needed. *N*-[Methyl-^{11}C]2-(4′-methylamino-phenyl)-6-hydroxybenzothiazole (^{11}C-PIB), a PET tracer developed for Alzheimer's disease, might also visualize deposition of amyloids in the heart [15]. PET has a higher spatial resolution than a planar image or SPECT and can be fused with CT for better anatomic resolution [5]. However, it is unclear whether ^{11}C-PIB PET is helpful to localize amyloidosis outside the heart.

There are several case reports and case series about ^{18}F-fluorodeoxyglucose positron emission tomography/computed tomography (^{18}F-FDG PET/CT). Although ^{18}F-FDG PET/CT has established its usefulness in the field of oncology, its imaging findings and clinical value in amyloidosis have not yet been clarified [13]. Therefore, we investigated the imaging findings and diagnostic efficacy of ^{18}F-FDG PET/CT in patients with primary systemic AL amyloidosis in various organs.

Materials and Methods

Subjects

From December 2006 to April 2013, 15 subjects with histologically confirmed systemic amyloidosis underwent pretreatment ^{18}F-FDG PET/CT and their medical records were retrospectively reviewed. Among them, nine patients had alleged malignancy (multiple myeloma in seven, lung cancer in one, and thyroid cancer in one).

In the 15 patients, 22 organs (10 hearts, 5 kidneys, 2 stomachs, 2 colons, 1 ileum, 1 pancreas, and 1 liver) were affected by AL amyloidosis. Six subjects were histologically confirmed to have multiple involved organs including heart, pancreas, stomach, colon, and kidney. In the remaining nine subjects, only one involved organ was pathologically indicated. Histology was also evaluated on pretreatment biopsy specimens. The median interval from ^{18}F-FDG PET/CT study to histologic review was 20 days (range 0–62). Our institutional review board approved the protocol of this retrospective study.

^{18}F-FDG PET/CT

All subjects who underwent ^{18}F-FDG PET scans at our institution fasted for at least 6 h beforehand. The range of blood glucose at the time of ^{18}F-FDG injection was 74–150 mg/dl. PET/CT scans were performed on two different dedicated PET/CT scanners (Discovery LS or Discovery STe; GE Healthcare, Milwaukee, WI, USA) from the skull base to mid-thigh without intravenous or oral contrast material. Two scans were conducted 60 min after the injection of ^{18}F-FDG (5.5 MBq/kg). Acquisition duration was 4 min per frame in two-dimensional (2D) mode in the Discovery LS and 2.5 min per frame in three-dimensional (3D) mode in the Discovery STe. Images were reconstructed with attenuation correction (CT-based). Whole-body CT was performed using a continuous spiral technique with an eight-slice helical CT (140 KeV, 40–120 mAs adjusted to the patients' body weight, section width of 5 mm) in the Discovery LS scanner and with a 16-slice helical CT (140 KeV, 30–170 mAs with AutomA mode, section width of 3.75 mm) in the Discovery STe scanner. Attenuation-corrected PET images (voxel size=3.9×3.9×3.3 mm) were reconstructed using CT data and a 3D ordered-subsets expectation maximization algorithm (20 subsets, 2 iterations) in the Discovery STe scanner and an ordered-subsets expectation maximization algorithm (28 subsets, 2 iterations) in the Discovery LS scanner. Commercial software (Advantage Workstation; GE Healthcare) was used to accurately co-register the separate CT and PET scan data.

Among the 15 patients, scans in 6 were performed using the Discovery LS PET/CT scanner, and scans in 9 patients were performed using the Discovery STe PET/CT scanner.

^{18}F-FDG PET/CT image analysis focused on the organs histopathologically confirmed as affected by amyloidosis. Retrospective visual analysis was performed by two nuclear medicine physicians. If hypermetabolic lesions were found, maximum SUV (SUVmax) was measured. Positive PET was defined as the presence of a focally or diffusely increased radioactive uptake higher than background, reference organ, or organ-specific physiologic uptake. For the liver, spleen activity was used as a reference organ. For kidneys, when there was no significantly high urine activity in the pelvicalyceal system, liver activity was used as a reference organ. For bowels, the activity of involved bowels confirmed by endoscopic biopsy and/or contrast-enhanced CT was evaluated. For hearts, to decrease the physiological uptake, strict fasting for more than 6 h and blood glucose level less than 150 mg/dl were achieved [16].

Literature Review

To compare with previous reports, bibliographic data were retrieved from the PubMed database using the following

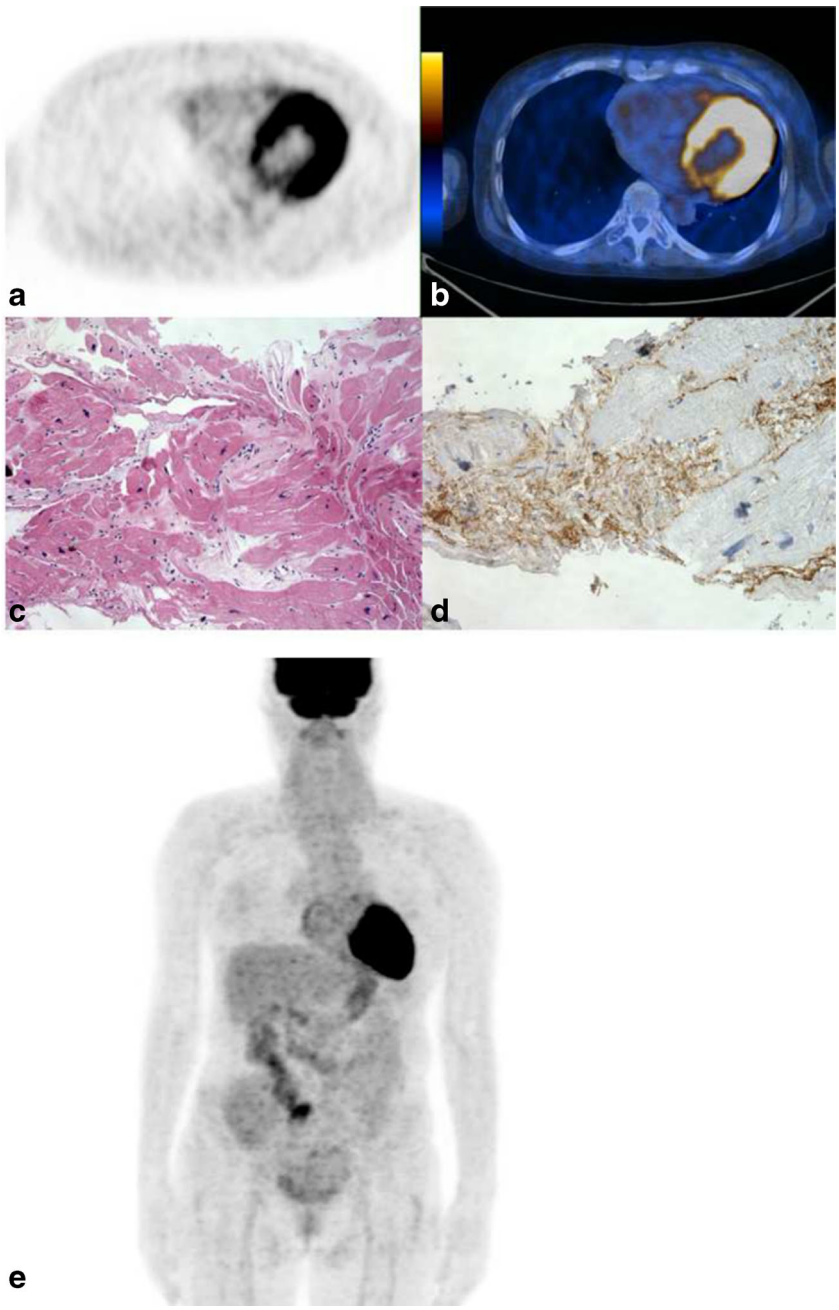

Fig. 1 Increased ^{18}F-FDG uptake along the epicardial side and great vessel with ventricular hypertrophy on transverse PET (**a**), fused PET/CT images (**b**) and maximum intensity projection (MIP) (**e**) in a 58-year-old female patient who complained of progressive dyspnea (SUVmax= 14.1). Pathological specimen obtained by cardiac biopsy revealed amyloid deposition in hematoxylin and eosin staining (**c**) and immunohistochemical staining for amyloid P protein (**d**)

keywords: amyloidosis, ^{18}F-FDG, and PET. Eventually, we chose 15 relevant articles for comparison with our study [4, 10, 13, 17–24]. Among them, we used pathologically proven AL amyloidosis results.

Statistical Analysis

Statistical analysis was performed using commercial software (SPSS Statistics, version 19; IBM, New York, NY). The Mann–Whitney *U* test was used for the comparison of two continuous variables. A p value<0.05 was considered statistically significant.

Results

Among the 15 patients with pathologically proven AL amyloidosis (M:F=12:3; age, 61.5±7.4 years), most had nonspecific symptoms, such as dyspnea, dizziness, generalized edema, or abdominal discomfort (3 with dyspnea, 2 with dizziness, 2 with generalized edema, and 4 with abdominal discomfort). One of them had experienced weight loss.

^{18}F-FDG uptake was significantly increased in 15 of the 22 organs (68.2 %; 10 hearts, 2 kidneys, 1 colon, 1 ileum, and 1 liver; SUVmax=7.0±3.2, range 2.1–14.1). None of the patients had a known infection or clinical signs of an infectious condition at the time of ^{18}F-FDG PET/CT. However, in 11 of

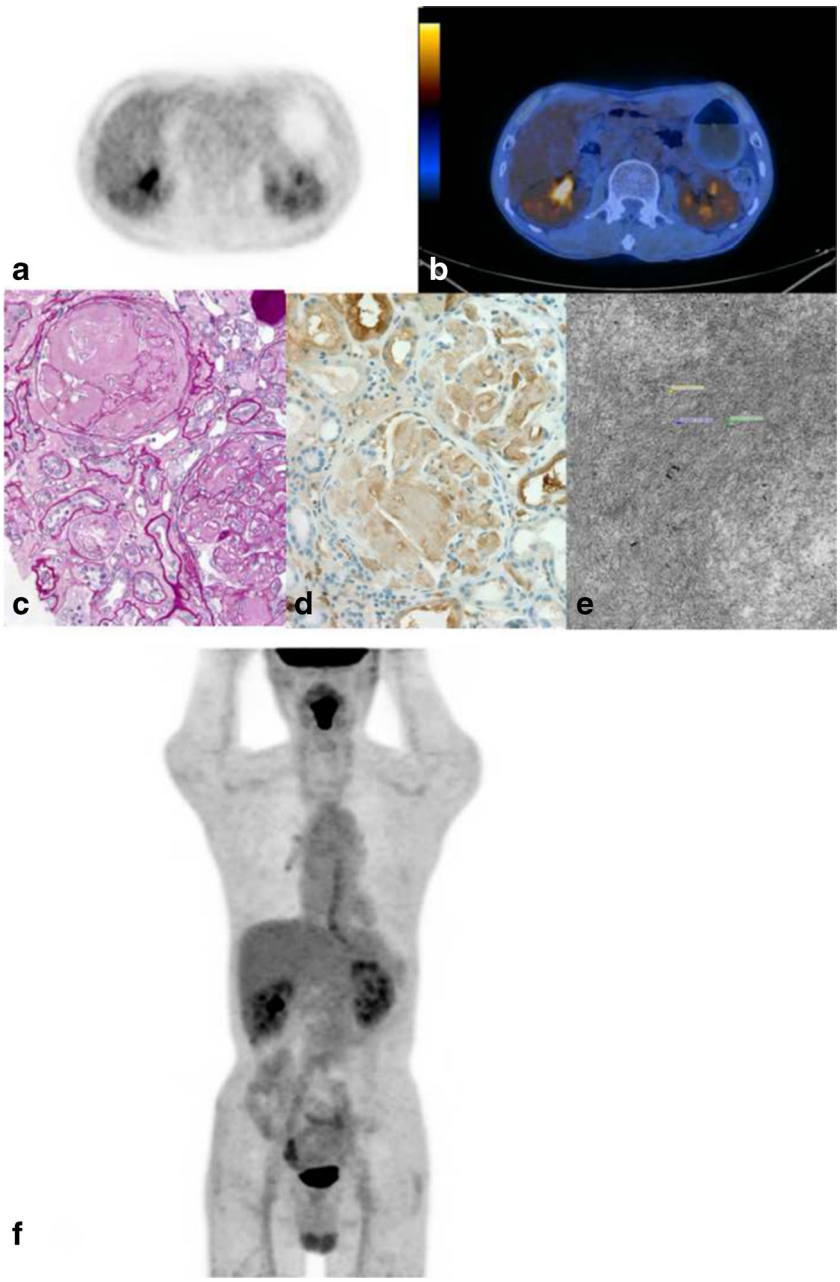

Fig. 2 Abnormal diffuse renal parenchymal ^{18}F-FDG uptake (SUVmax=3.5) on transverse PET (**a**), fused PET/CT images (**b**) and MIP (**f**) in a 61-year-old male patient with biopsy-proven bilateral renal amyloidosis. Pathological specimen obtained by renal biopsy revealed amyloid deposition in periodic acid Schiff staining (**c**), immunohistochemical staining for anti-lambda antibody (**d**) and electron microscopy showing interlacing bundles of parallel arrays of fibrils with a diameter of 11–13 nm (**e**)

Table 1 Clinical and ^{18}F-FDG PET/CT data of patients with biopsy-proven AL amyloidosis before treatment

Subjects	Age (years)	Sex	Symptoms	Involved organ	^{18}F-FDG PET/CT uptake pattern (SUVmax)	Other image findings
Case 1	55	M	Cramping abdominal pain, hematochezia	Heart	Diffuse myocardial uptake (LV=7.4, LA=2.9, RV=3.9, RA=3.4)	**Echocardiogram** Mild LV/RV systolic dysfunction Increased LV and RV wall thickness Atrial enlargement Pericardial effusion
				Stomach	NA	
				Colon	NA	
Case 2	65	M	Dyspnea, dizziness, abdominal discomfort	Heart	Diffuse myocardial uptake (LV=8.1, RV=3.4, RA=2.9)	**Abdomen and pelvis CT** Extensive lymphadenopathy in the left gastric, hepatoduodenal, and peripancreatic areas Bilateral pleural effusion
				Pancreas	NA	
Case 3	55	M	Weight loss	Heart	Diffuse myocardial uptake (LV=7.2, RV=2.7, RA=2.4)	**Cardiac MR** Diffuse myocardial hypertrophy with subtle myocardial increased signal intensity on T2WI Subendocardial enhancement on delayed enhancement image
				Kidney	NA	**Kidney US** Unremarkable findings
Case 4	43	M	Azotemia	Heart	Diffuse myocardial uptake (LV=12.0, LA=3.3, RV=6.8, RA=2.6)	**Echocardiogram** Increased LV and RV wall thickness Atrial enlargement Dilated pulmonary artery Loculated pericardial effusion Large amount of pleural effusion
				Kidney	Diffuse parenchymal uptake, both (2.1)	**Kidney US** Heterogeneously increased echogenicity of both kidneys Ascites and bilateral pleural effusions
Case 5	68	F	Diarrhea	Heart	Diffuse myocardial uptake (LV=7.0, RV=2.5, RA=2.5)	**Echocardiogram** Increased basal septal and RV wall thickness Minimal amount of pericardial effusion
				Colon	Diffuse heterogeneous (4.0)	**Abdomen and pelvis CT** Layered wall thickening involving small and large bowel
Case 6	56	M	Dyspnea, generalized edema	Heart	Diffuse myocardial uptake (LV=5.5, LA=2.1, RV=6.7, RA=3.3)	**Echocardiogram** Borderline thickened LV wall with sparkling Minimal pericardial effusion without hemodynamic compromise
Case 7	57	M	None	Heart	Diffuse myocardial uptake (LV=14.1, LA=3.5, RV=6.7, RA=3.1)	**Cardiac MR** Restrictive physiology and multifocal delayed enhancement of LV wall thickening
Case 8	68	M	None	Heart	Diffuse myocardial uptake (LV=6.6, LA=4.8, RV=5.6, RA=2.8)	**Cardiac MR** Concentric myocardial hypertrophy with delayed hyper-enhancement Decreased systolic function (ejection fraction; 27 %). Right pleural effusion
Case 9	60	F	Dizziness, syncope	Heart	Diffuse myocardial uptake (LV=6.0, RV=4.0)	**Echocardiogram** Increased LV and RV wall thickness Diastolic dysfunction grade 2 with LA enlargement Pericardial and pleural effusion

Table 1 (continued)

Subjects	Age (years)	Sex	Symptoms	Involved organ	^{18}F-FDG PET/CT uptake pattern (SUVmax)	Other image findings
Case 10	74	M	None	Heart	Diffuse myocardial uptake (LV=5.9, RV=3.3, RA=3.0)	**Echocardiogram** Increased LV and RV wall thickness Slightly decreased RV systolic function Diastolic dysfunction grade 2 with biatrial enlargement Pericardial effusion
Case 11	63	M	Nausea, vomiting	Stomach Kidney	NA Diffuse parenchymal uptake, both (3.5)	**Abdomen and pelvis CT** Unremarkable finding
Case 12	53	M	Proteinuria	Kidney	NA	
Case 13	69	M	Generalized edema	Kidney	NA	
Case 14	62	M	Dyspnea, abdominal pain	Terminal ileum	Diffuse intestinal wall uptake (5.5)	**Abdomen and pelvis CT** Small bowel wall thickening and enhancement Ascites and bilateral pleural effusions
Case 15 [8]	65	F	Lower abdominal pain	Liver	Diffuse uptake (10.9)	**Abdomen and Pelvis CT** Hepatomegaly with heterogeneous hepatic enhancement Ascites
Sum				22	13 (59.09 %) (SUVmax=7.04, range 2.1 – 14.1)	

^{18}F-FDG PET/CT ^{18}F-fluorodeoxyglucose positron emission tomography/computed tomography, *SUVmax* maximum standardized uptake value, *M* male, *F* female, *LV* left ventricle, *Sum* summation, *NA* not applicable

15 PET-positive organs (73.3 %; 10 hearts and the ileum), it was difficult to differentiate physiological uptake from pathological uptake.

In all ten patients with cardiac involvement, diffuse increased ^{18}F-FDG uptake was found along the myocardium. The most ^{18}F-FDG-avid sites were the left ventricle (LV) (n=10, SUVmax=8.0±2.7, range 5.5–14.1), followed by the right ventricle (RV) (n=10, SUVmax=4.2±1.6, range 2.4–6.8), right atrium (RA) (n=9, SUVmax=2.7±0.6, range 2.4–3.4) and left atrium (LA) (n=5, SUVmax=2.1±1.3, range 2.1–4.8). Among those ten patients, seven had cardiac wall thickening in cardiac MRI or echocardiogram; three had thickening in both ventricular walls, three had a borderline-thickened LV wall, and one had basal septal and RV wall thickness. The subgroup with cardiac wall thickening appeared to have higher ^{18}F-FDG uptake than patients without cardiac wall thickening, although the difference was not significant (SUVmax, 8.54±3.2 vs 6.67±1.3, p=0.43). Eight of ten subjects with cardiac involvement had mild to moderate pericardial or pleural effusion (pericardial effusion in four, pleural effusion in two, and both in two). Despite these findings, diffuse ^{18}F-FDG uptake in the heart can also be seen in normal myocardium, so-called physiological uptake. Because myocardial uptake of ^{18}F-FDG is heterogeneously based on metabolic shifts in myocardial cells [25], differentiation between physiological uptake and pathological uptake was very difficult. A representative case is displayed in Fig. 1. In the ileum, mildly increased ^{18}F-FDG uptake (SUVmax=5.5) along the wall with segmental wall thickening and enhancement were seen in contrast abdominal CT image. However, it was difficult to differentiate that uptake from physiological bowel uptake based on the PET/CT alone.

Except for those organs, definitely abnormal ^{18}F-FDG uptake was found in only 4 of the 22 organs (18.2 %; 2 kidneys, 1 liver, 1 colon). In the kidneys, there was diffusely increased renal parenchymal ^{18}F-FDG uptake compared with liver activity without significant physiological urine activity in the pelvicalyceal system (Fig. 2). In the liver, there was markedly heterogeneous increased ^{18}F-FDG uptake in the hepatic parenchyma with hepatomegaly, which was previously published as a case report [7]. In the colon, persistent wall thickening was noted in an enhanced abdomen and pelvis CT. Initially, the patient presented to the hospital due to diarrhea. After loosening the bowel, layered wall thickening involving the small and large bowel was still noted. The clinician performed a biopsy and diagnosed amyloidosis (SUVmax=4.0). PET was negative for all pancreas and gastric lesions. These data are summarized in Table 1.

During clinical follow-up, nine subjects died: three during diagnostic workup and the other six during clinical follow-up after therapy for amyloidosis. The causes of death were progression of multiple myeloma in four, heart failure in one, pneumonia in 1, hepatic failure in one, renal failure in one, and malignancy in one. In the deceased group, the mean

Table 2 ^{18}F-FDG PET-CT in amyloidosis (literature data)

Organ	Number of organs	Positive FDG PET	Sensitivity of PET (%)	SUVmax
Lung [7, 13, 15–17, 20–22, 31, 32]	17	11	64.7	7 (range 1.8–7)
Nasopharynx [13, 23]	4	4	100	15 (range 4–15)
Muscle [7, 12, 13]	3	3	100	8 (range 8)
Heart [7, 13]	6	0	0	NA
Joint [7, 13, 19]	3	3	100	8 (range 8)
Skin [7, 13]	2	2	100	9 (range 9)
Bone/bone marrow [7, 12]	4	1	25.0	NA
Intestine [7, 13, 18]	3	2	66.7	NA
Kidney [7, 13]	6	0	0	NA
Liver [7, 13]	3	0	0	NA
Sum	51	26	50.98	9.4 (range 1.8–15)

SUVmax (7.9, range 5.5–14.1) of amyloidosis-involved organs was higher than that (5.1, range 1.0–12.0) for the surviving group, with borderline statistical significance (p=0.15).

In all six subjects without history of malignancy, no other abnormal findings, such as malignancy, were found on the ^{18}F-FDG PET/CT. During follow-up (17.6±11.3 months after PET/CT), no clinical evidence suggested new malignancy in those patients. In the literature review, among 15 previously reported ^{18}F-FDG PET/CT cases and 34 amyloidosis-involved organs, PET/CT was positive in 26 organs (51.34 %) and showed a median SUVmax of 9.4 (range 1.8–15.0), which was similar to our findings. The involved organs in the literature included lung (n=17), nasopharynx (n=4), muscle (n=3), heart (n=6), joint (n=3), skin (n=2), bone (n=1), intestine (n=3), kidney (n=6), liver (n=3) and bone marrow (n=3). Characteristics of organs in the literature data are listed in Table 2.

To summarize our data and the literature data, ^{18}F-FDG PET/CT was positive in 39 organs (53.4 %) and showed a median SUVmax of 9.0 (range 1.8–14.3). These data are summarized in Table 3. ^{18}F-FDG uptake in the 39 organs with positive PET/CT was observed in the lung (n=11), nasopharynx (n=4), muscle (n=3), heart (n=9), joint (n=3), skin (n=2), kidney (n=1), intestine (n=3), bone marrow (n=1) and liver (n=1). ^{18}F-FDG uptake was absent in bone (n=1), pancreas (n=1), and stomach (n=1).

Discussion

^{18}F-FDG PET has been considered a reliable method in oncology, including the detection of active multiple myeloma, which is one of the plasma cell dyscrasias; however, evidence of its diagnostic power in amyloidosis remains lacking [13, 26]. AL amyloidosis, formerly called primary amyloidosis, occurs in patients with B-cell or plasma-cell dyscrasias in whom fragments of monoclonal immunoglobulin light chains

Table 3 Summary of ^{18}F-FDG PET/CT results in AL amyloidosis, including our data and literature data

Organ	Number of organs	Positive FDG PET	Positivity of PET (%)	SUVmax
Lung	17	11	64.7	7 (range 1.8–7)
Nasopharynx	4	4	100	15 (range 4–15)
Muscle	3	3	100	8 (range 8)
Heart	16	10	62.5	14.1 (range 5.5–14.1)
Joint	3	3	100	8 (range 8)
Skin	2	2	100	9 (range 9)
Bone/bone marrow	4	1	25.0	NA
Intestine	8	3	37.5	5.5 (range 4.0–5.5)
Kidney	11	1	8.3	3.5
Liver	4	1	25	10.9
Pancreas	1	0	0	NA
Sum	73	39	50.32	9.0 (range 1.8–14.3)

form amyloid fibrils [27]. Plasma cell malignancies are characterized by clonal expansion of terminally differentiated B lymphoid cells, usually resulting in the production of a monoclonal immunoglobulin protein [28]. Although the relevance of bone marrow plasmacytosis in amyloidosis is not always clear, a spectral overlap between AL amyloidosis and myeloma is not uncommon [28]. Nevertheless, despite favorable ^{18}F-FDG uptake in multiple myeloma, the avidity of FDG in systemic AL amyloidosis is variable.

In our study, the sensitivity was not high (68.2 %). Furthermore, it was difficult to differentiate pathological uptake from physiological uptake in the involved organs, especially in cases involving the heart and kidneys. Although adequate fasting before PET/CT scan was performed in all cases in order to prevent physiological cardiac uptake, it could not be certain that the diffuse cardiac uptake we observed was pathological because the uptake pattern was similar to physiological uptake influenced by blood flow, ischemia, and hormonal control as well as fasting [29, 30]. Variable ^{18}F-FDG uptake in systemic AL amyloidosis might be partly explained by the absence of giant cells and other inflammatory cells, which show high ^{18}F-FDG uptake compared with localized amyloidosis [4].

According to our data and literature review, significant ^{18}F-FDG uptake was noted in almost 50.3 % of organs involving AL amyloidosis. In particular, high sensitivity was found in heart, lung, muscle, joint, skin, and nasopharynx with AL amyloidosis (Table 3). Considering physiological uptake, ^{18}F-FDG PET/CT may be helpful to diagnosis amyloidosis in lung, muscle, joint, skin, and nasopharynx, because those organs show no or mild-to-moderate physiological uptake. On the contrary, ^{18}F-FDG PET/CT showed poor sensitivity in bone/bone marrow, intestine, liver, and kidney (Table 3). Because clinical manifestation of AL amyloidosis is nonspecific, such as fatigue and unintentional weight loss, it is necessary to exclude other pathological conditions such as malignancy. In our study, six subjects underwent ^{18}F-FDG PET/CT that showed no abnormal uptake suggesting malignancy. During clinical follow-up of those patients, none was diagnosed with new malignancy. Therefore, ^{18}F-FDG PET/CT may be helpful to rule out other diseases, such as malignancy.

This study had several limitations. First, the number of subjects was small, despite being larger than in previous studies. Second, pathological confirmation was performed in only some of the suspected organs because of a retrospective design and ethical restrictions. Therefore, we could not determine a definitive specificity of ^{18}F-FDG PET/CT for detecting AL amyloidosis. Third, two different kinds of ^{18}F-FDG PET/CT scanners and acquisition protocols were used; therefore, the SUVmax comparisons might be imprecise. Lastly, we investigated only pathologically confirmed organs because as yet there are no widely available validated non-invasive diagnostic criteria for the involved organs. Therefore, there might be other organs involving amyloidosis.

Conclusions

Significantly high ^{18}F-FDG uptake was present in about two-thirds of organs involved in systemic AL amyloidosis. However, in involved organs that frequently show physiological uptake, it might be difficult to evaluate involvement of amyloidosis using ^{18}F-FDG PET/CT alone. ^{18}F-FDG PET/CT may be helpful for ruling out other diseases, especially malignancy. Because of small number of subjects and lack of follow-up ^{18}F-FDG PET/CT after treatment, further studies are warranted to evaluate the role of ^{18}F-FDG PET/CT in systemic AL amyloidosis.

Acknowledgments This work was supported by the Research Program funded by the Korean Centers for Disease Control and Prevention (2013-E63011-00).

Conflict of Interest The authors, Joo Hee Lee, Ga Yeon Lee, Seok Jin Kim, Ki Hyun Kim, Eun-Seok Jeon, Kyung-Han Lee, Byung-Tae Kim and Joon Young Choi, declare that they have no conflicts of interest.

Ethical Statement Our study was done in compliance with the regulations of our institution and generally accepted guidelines governing such work. Each author has participated sufficiently in the work to take responsibility for the contents. We warrant that this manuscript is original, is not under simultaneous consideration by another journal, and has not been previously published. And there are no financial associations that might cause a conflict of interest.

References

1. Pepys MB. Pathogenesis, diagnosis and treatment of systemic amyloidosis. Philos Trans R Soc Lond B Biol Sci. 2001;356:203–10. discussion 10–1.
2. Glaudemans AW, Slart RH, Zeebregts CJ, Veltman NC, Tio RA, Hazenberg BP, et al. Nuclear imaging in cardiac amyloidosis. Eur J Nucl Med Mol Imaging. 2009;36:702–14.
3. Lobato L, Rocha A. Transthyretin amyloidosis and the kidney. Clin J Am Soc Nephrol. 2012;7:1337–46.
4. Glaudemans AW, van Rheenen RW, van den Berg MP, Noordzij W, Koole M, Blokzijl H, et al. Bone scintigraphy with ^{99m}technetium-hydroxymethylene diphosphonate allows early diagnosis of cardiac involvement in patients with transthyretin-derived systemic amyloidosis. Amyloid. 2014;21:35–44.
5. Baqir M, Lowe V, Yi ES, Ryu JH. ^{18}F-FDG PET scanning in pulmonary amyloidosis. J Nucl Med. 2014;55:565–8.
6. Hachulla E, Grateau G. Diagnostic tools for amyloidosis. Joint Bone Spine. 2002;69:538–45.
7. Glaudemans AW, Slart RH, Noordzij W, Dierckx RA, Hazenberg BP. Utility of ^{18}F-FDG PET(/CT) in patients with systemic and localized amyloidosis. Eur J Nucl Med Mol Imaging. 2013;40:1095–101.
8. Son YM, Choi JY, Bak CH, Cheon M, Kim YE, Lee KH, et al. ^{18}F-FDG PET/CT in primary AL hepatic amyloidosis associated with multiple myeloma. Korean J Radiol. 2011;12:634–7.
9. Aljaroudi WA, Desai MY, Tang WH, Phelan D, Cerqueira MD, Jaber WA. Role of imaging in the diagnosis and management of patients with cardiac amyloidosis: State of the art review and focus on emerging nuclear techniques. J Nucl Cardiol. 2014;21:271–83.
10. de Haro-del Moral FJ, Sanchez-Lajusticia A, Gomez-Bueno M, Garcia-Pavia P, Salas-Anton C, Segovia-Cubero J. Role of cardiac

scintigraphy with ^{99m}Tc-DPD in the differentiation of cardiac amyloidosis subtype. Rev Esp Cardiol (Engl Ed). 2012;65:440–6.
11. Rapezzi C, Quarta CC, Guidalotti PL, Pettinato C, Fanti S, Leone O, et al. Role of ^{99m}Tc-DPD scintigraphy in diagnosis and prognosis of hereditary transthyretin-related cardiac amyloidosis. JACC Cardiovasc Imaging. 2011;4:659–70.
12. Seo JH, Lee SW, Ahn BC, Lee J. Pulmonary amyloidosis mimicking multiple metastatic lesions on ^{18}F- FDG PET/CT. Lung Cancer. 2010;67:376–9.
13. Mekinian A, Jaccard A, Soussan M, Launay D, Berthier S, Federici L, et al. ^{18}F-FDG PET/CT in patients with amyloid light-chain amyloidosis: case-series and literature review. Amyloid. 2012;19:94–8.
14. Jeong J, Kong E, Chun K, Cho I. The impact of energy substrates, hormone level and subject-related factors on physiologic myocardial ^{18}F-FDG uptake in normal humans. Nucl Med Mol Imaging. 2013;47:225–31.
15. Costantino F, Loeuille D, Dintinger H, Pere P, Chary-Valckenaere I. Fixed digital contractures revealing light-chain amyloidosis. Joint Bone Spine. 2009;76:553–5.
16. Grubstein A, Shitrit D, Sapir EE, Cohen M, Kramer MR. Pulmonary amyloidosis: detection with PET-CT. Clin Nucl Med. 2005;30:420–1.
17. Kung J, Zhuang H, Yu JQ, Duarte PS, Alavi A. Intense fluorodeoxyglucose activity in pulmonary amyloid lesions on positron emission tomography. Clin Nucl Med. 2003;28:975–6.
18. Mainenti PP, Segreto S, Mancini M, Rispo A, Cozzolino I, Masone S, et al. Intestinal amyloidosis: two cases with different patterns of clinical and imaging presentation. World J Gastroenterol. 2010;16:2566–70.
19. Mekinian A, Ghrenassia E, Pop G, Roberts S, Prendki V, Stirnemann J, et al. Visualization of amyloid arthropathy in light-chain systemic amyloidosis on ^{18}F-FDG PET/CT scan. Clin Nucl Med. 2011;36:52–3.
20. Ollenberger GP, Knight S, Tauro AJ. False-positive FDG positron emission tomography in pulmonary amyloidosis. Clin Nucl Med. 2004;29:657–8.
21. Tan H, Guan Y, Zhao J, Lin X. Findings of pulmonary amyloidosis on dual phase FDG PET/CT imaging. Clin Nucl Med. 2010;35:206–7.
22. Yadav S, Sharma S, Gilfillan I. Unusual positron emission tomography findings in pulmonary amyloidosis: a case report. J Cardiothorac Surg. 2006;1:32.
23. Yoshida A, Borkar S, Singh B, Ghossein RA, Schoder H. Incidental detection of concurrent extramedullary plasmacytoma and amyloidoma of the nasopharynx on ^{18}F-fluorodeoxyglucose positron emission tomography/computed tomography. J Clin Oncol. 2008;26:5817–9.
24. Morooka M, Moroi M, Uno K, Ito K, Wu J, Nakagawa T, et al. Long fasting is effective in inhibiting physiological myocardial ^{18}F-FDG uptake and for evaluating active lesions of cardiac sarcoidosis. EJNMMI Res. 2014;4:1.
25. Hawkins PN, Lavender JP, Pepys MB. Evaluation of systemic amyloidosis by scintigraphy with ^{123}I-labeled serum amyloid P component. N Engl J Med. 1990;323:508–13.
26. Wei A, Juneja S. Bone marrow immunohistology of plasma cell neoplasms. J Clin Pathol. 2003;56:406–11.
27. Iozzo P, Chareonthaitawee P, Di Terlizzi M, Betteridge DJ, Ferrannini E, Camici PG. Regional myocardial blood flow and glucose utilization during fasting and physiological hyperinsulinemia in humans. Am J Physiol Endocrinol Metab. 2002;282:E1163–71.
28. Dutka DP, Pitt M, Pagano D, Mongillo M, Gathercole D, Bonser RS, et al. Myocardial glucose transport and utilization in patients with type 2 diabetes mellitus, left ventricular dysfunction, and coronary artery disease. J Am Coll Cardiol. 2006;48:2225–31.
29. Hazenberg BP, van Rijswijk MH, Lub-de Hooge MN, Vellenga E, Haagsma EB, Posthumus MD, et al. Diagnostic performance and prognostic value of extravascular retention of ^{123}I-labeled serum amyloid P component in systemic amyloidosis. J Nucl Med. 2007;48:865–72.
30. Park CH, Kim HS, Shin HY, Kim HC. Hepatic uptake of Tc-99 m MDP on bone scintigraphy from intravenous iron therapy (Blutal). Clin Nucl Med. 1997;22:762–4.
31. Currie GP, Rossiter C, Dempsey OJ, Legge JS. Pulmonary amyloid and PET scanning. Respir Med. 2005;99:1463–4.
32. Soussan M, Ouvrier MJ, Pop G, Galas JL, Neuman A, Weinmann P. Tracheobronchial FDG uptake in primary amyloidosis detected by PET/CT. Clin Nucl Med. 2011;36:723–4.